



EPR Spectroscopy of the Ground Electron State of the Fe²⁺ Impurity Ion in Amethyst

V. F. Tarasov¹ · R. B. Zaripov¹

Received: 28 June 2024 / Revised: 10 July 2024 / Accepted: 11 July 2024 /
Published online: 16 July 2024

© The Author(s), under exclusive licence to Springer-Verlag GmbH Austria, part of Springer Nature 2024

Abstract

Properties of two lowest electron levels of the Fe²⁺ impurity ion in a natural amethyst are studied by continuous wave electron paramagnetic resonance spectroscopy in the Q-band. It is established that these levels present quasi-doublet $|\pm 2\rangle$ with zero-field splitting of 30.9 ± 0.2 GHz. Orientation of principal magnetic axes and value of *g*-factor of this paramagnetic center are determined.

1 Introduction

During the 80 years since the discovery by E.K. Zavoisky of the electron paramagnetic resonance (EPR) in condensed matter, EPR spectroscopy has proved to be one of the most effective methods to study valence state and localization in the crystal lattice of 3d and 4f impurity ions in dielectric crystals. The information obtained in this case turned out to be very important, since these characteristics largely determine the most important optical properties of crystals, including their color, efficiency and lifetime of luminescence, efficiency of laser generation, and so on. In this article, we used EPR spectroscopy to study Fe²⁺ impurity ions in natural amethyst from the Pamir deposit.

Amethyst is a well-known violet colored kind of quartz (SiO₂). Usually, this color is attributed to the presence in crystals of impurity Fe⁴⁺ ions. The precursor of this center is a Fe³⁺ ion substituting Si⁴⁺ in the tetrahedral position [1–3]. When the amethyst crystal is exposed by γ -radiation, Fe³⁺ ions substituting Si⁴⁺ in tetrahedral environment lose an electron and turn into a Fe⁴⁺ ion, creating a characteristic amethyst color. It has been noted in a number of articles that simultaneously absorption bands characteristic for Fe²⁺ ions appear in the optical spectra. It is assumed that the interstitial Fe³⁺ ions, localized in channels parallel or perpendicular to the

✉ V. F. Tarasov
tarasov@kfti.knc.ru

¹ Zavoisky Physical-Technical Institute, Federal Research Center “Kazan Scientific Center of RAS”, Kazan 420029, Russia

crystallographic c -axis, turn into the Fe^{2+} state under ionizing radiation [4–6]. The role of the Fe^{2+} ions in the formation of the characteristic color of amethyst was discussed in the articles [5, 7, 8]. Later, the identification of the valence state of iron in amethyst and role of divalent iron in amethyst coloration were investigated by X-ray absorption [9, 10] and Mössbauer spectroscopy [11, 12]. Application of EPR spectroscopy for the characterization of two- and four-valent iron ions in low symmetry crystal field is not very efficient due to the peculiarities of the fine structure of the electron levels. The ground electron states of these $3d^4$ and $3d^6$ ions have 4 electrons or holes on the 3d shell, respectively, with the total spin $S=2$. The low symmetry electric crystal field of amethyst splits the spin levels into five singlets. The large value of the energy gap between these singlet levels makes it difficult to observe resonance transitions between them using conventional X-band EPR spectrometers with an operating frequency of about 10 GHz. For the Fe^{4+} ion, the only resonance transition between the levels of the quasi-doublet $|\pm 2\rangle$ was observed [13] at frequencies of 16 and 35 GHz. This made it possible to measure zero field splitting between the quasi-doublet levels. Other parameters of the fine structure of the ground electron state of Fe^{4+} impurity ions in amethyst were measured in the article [14] using a broadband frequency-tunable spectrometer [15]. In the article [14], EPR spectra of Fe^{4+} were observed after γ -irradiation of the sample with a dose of about 30 Mrad using a ^{60}Co source. As a consequence, the intensity of the EPR line of the Fe^{4+} ions increased several times. At the same time, resonance lines of another non-Kramer paramagnetic center appeared on the spectra. The study of its characteristics led us to the conclusion that these lines belong to a Fe^{2+} ion with interstitial localization in one of the channels.

2 Sample and Experiment Details

The measurements were carried out in the Q-band on an ELEXSYS E580 spectrometer (34 GHz) at temperature 20 K. The spectrometer was equipped with a commercial resonator ER5106QTW (with TE011 wave mode), which was placed into a CF935 cryostat. The temperature was controlled using an ITC 503 temperature controller (Oxford). To measure orientation dependencies of resonance transitions, we used a programmable single-axis goniometer ER218PG1 (Bruker) with a resolution of 0.125° and a working range of 360°. A sample of natural amethyst originated from the Pamir deposit was studied. Measurements were carried out with the sample of about $1 \times 1 \times 1 \text{ mm}^3$. According to the data of X-ray fluorescence analysis, in addition to silicon and oxygen, the sample contained the following elements (as a percentage relative to ^{28}Si): ^{20}Ca , 0.04; ^{16}S , 0.09; ^{19}K , 0.03, ^{56}Fe , 0.02. The SiO_2 crystal has a trigonal structure at room temperature and belongs to the enantiomorphic space groups $P3_121 (D3_2^4)$ or $P3_221 (D3_2^6)$. There is one screw threefold axis (c -axis) and three twofold axes in the plane perpendicular to the threefold axis. This assumes the presence of at least three magnetically nonequivalent monoclinic centers for impurity paramagnetic centers, for which the projections of the principal magnetic axes on the plane perpendicular to the c -axis are rotated by 120 degrees.

3 Results and Discussion

We attribute new resonance lines that appear in spectra after γ -irradiation to the Fe²⁺ ions. These lines are much wider than other lines belonging to various transitions between the spin levels of the Fe³⁺ ions. Parameters of the Fe³⁺ impurity centers in amethyst can be found in the review article of Weil [16]. Spectra recorded at different frequencies of the microwave generator are presented in Fig. 1a. Frequency-field dependencies of these transitions are presented in Fig. 1b. It should be noted that the search for other resonance transitions belonging to this paramagnetic center in the frequency range up to 500 GHz using the broadband EPR spectrometer [15] did not yield positive results. Therefore, there is a reason to believe that the energies of other electron levels of this ion significantly exceed the value of zero field splitting between the levels of the ground quasi-doublet $|\pm 2\rangle$, and the states of this quasi-doublet do not mix with the states of the above electron levels. Then, we can assume that $g_x = g_y = 0$ for the non-Kramers ions with integer spin [17], and the simple spin Hamiltonian for effective electron spin $S = 1/2$ can be used to describe the frequency-field dependencies of the resonance transitions.

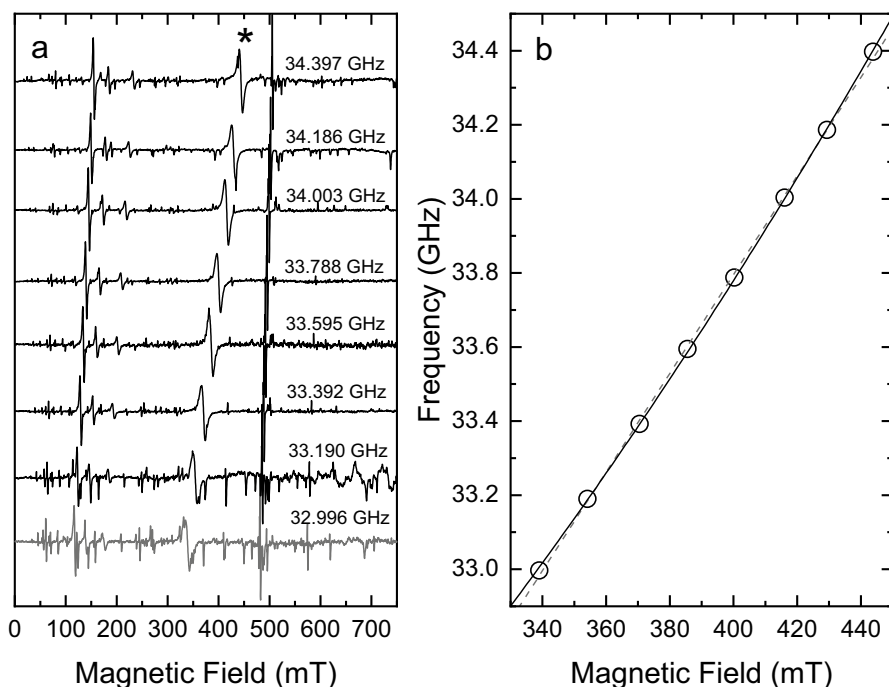


Fig. 1 Frequency-field dependency of resonant transitions of Fe²⁺ ion in amethyst. **a** spectra recorded at different frequencies of the microwave generator indicated on the right side of the spectra. Asterisk marks the line belonging to the Fe²⁺ ion; **b** experimental data (circles) and results of fitting using Eq. (2) (solid line). Linear dependency is presented by the dashed line for the comparison

$$H_{\text{eff}} = \Delta S_x + g_z^{\text{eff}} \mu_B B_z S_z. \quad (1)$$

Here, the first term corresponds to the zero-field splitting Δ between the quasi-doublet levels; the second term corresponds to the electron Zeeman energy. Effective g-factor $g_z^{\text{eff}} = mg_z$, where $m = 2$ or $m = 4$ for transitions between levels of quasi-doublets $|\pm 1\rangle$ and $|\pm 2\rangle$, respectively. The frequency of transitions between these levels may be calculated analytically for an arbitrary orientation of the magnetic field

$$\nu = \sqrt{\Delta^2 + (g_z^{\text{eff}} \mu_B B \cos \theta)^2}, \quad (2)$$

where θ is the angle between the direction of the magnetic field and the z axis of the paramagnetic center. To determine the value of Δ , Eq. (2) was used to describe the experimental data presented in Fig. 1. The best correspondence between theory and experiment was obtained at values $\Delta = 30.9$ GHz and $g_z^{\text{eff}} = 8.42$. The calculated non-linear dependency is shown in Fig. 1b by the solid line. Additionally, the experimental data were approximated by linear dependency. The dashed line shows this dependency obtained with the parameters $\Delta = 28.5$ GHz and $g_z^{\text{eff}} = 0.952$. The standard error with the description by Eq. (2) was $2.72 \cdot 10^{-5}$, and with linear dependency $1.2 \cdot 10^{-4}$. This confirms that these resonance lines belong to a non-Kramer paramagnetic center.

To determine the value of the g-factor and the orientation of the principal magnetic axes the orientation dependencies of the spectra were measured. They are shown in Fig. 2. These measurements indicated the presence of six magnetically nonequivalent centers. The intensities of resonant transitions of different centers were essentially different. This is due to the asymmetric distribution of impurity iron ions on various structurally equivalent but magnetically nonequivalent crystallographic positions. The same phenomenon was previously observed for the impurity Fe^{3+} ions [1, 2] and Fe^{4+} ions [13] in amethyst. Therefore, we were unable to reliably identify the transitions belonging to Fe^{2+} ions in all six magnetically nonequivalent positions. Figure 2 shows experimental data on the most intensive resonance transitions. Three magnetically nonequivalent centers are visible in Fig. 2a under rotation of magnetic field around the crystallographic c -axis. This corresponds to the symmetry of the SiO_2 crystal lattice, where the c -axis is the screw threefold axis. The projections of the principal magnetic z -axes on the rotation plane are perpendicular to the twofold symmetry axes of amethyst crystal lattice. Figure 2b indicates that the principal magnetic axes of the four visible magnetically nonequivalent centers are deflected from the crystal c -axis. If the axis of the sample rotation was perpendicular to the c -axis, the resonance lines of these four centers on Fig. 2b should coincide in pairs. It is not so in our case. The theoretical dependencies calculated using Eq. (2) and presented in Fig. 2 were obtained taking into account the nonzero value δ of the deviation of the axis of the sample rotation from the crystallographic plane (0001). The value of δ was included as a fitting parameter for both orientation dependencies. The best

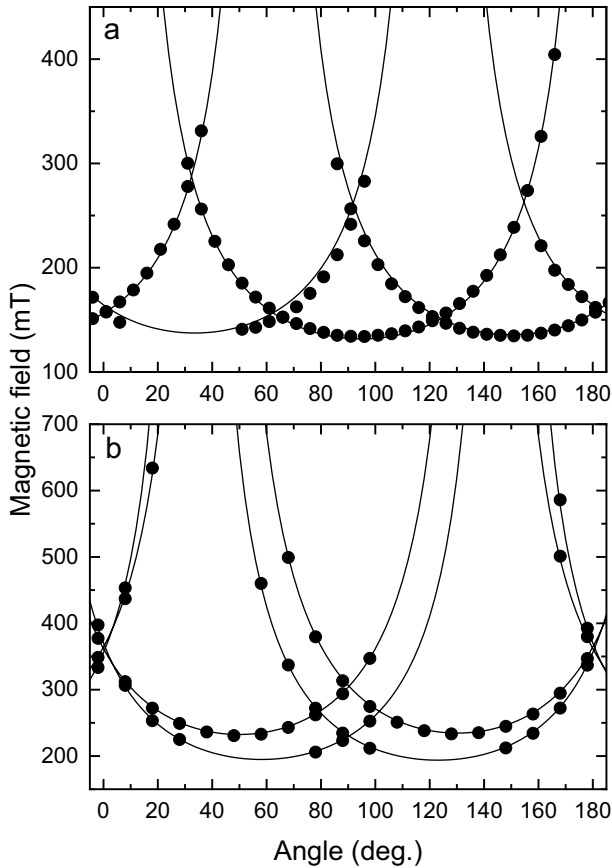


Fig. 2 Orientation dependencies of resonance transitions of Fe²⁺ ion in amethyst. Circles are experimental data, lines are theoretical dependences calculated using Eq. (2). The spectrometer frequency is 34.3 GHz

coincidence of experimental data and theoretical dependencies was obtained at the value of $g_z^{\text{eff}} = 8.5 \pm 0.2$. The angle of deviation of the principal z -axes of the centers from the c -axis equals $\beta = 70 \pm 0.5^\circ$. The values of δ equal to 7° and to 4.5° for the rotation of the magnetic field around the c -axis and in the perpendicular plane, respectively. The value of $g_z^{\text{eff}} = 8.5$ in Eq. (2) corresponds to the value of $g_z = 2.125$ for the resonance transition between the levels of the quasi-doublet $|\pm 2\rangle$. This value ($g_z > 2$) indicates that the spin-orbit coupling constant of this center is negative, i.e. the number of electrons on the d shell is more than five. This corresponds to the Fe²⁺ ion with 6 electrons on the d-shell.

4 Conclusion

Continuous wave EPR spectroscopy in the Q-band was used to study new non-Kramers paramagnetic center created in natural amethyst by γ -irradiation. We believe that this center is Fe^{2+} ion with an interstitial location. Observed resonance lines are due to transitions between electron levels of the ground quasi-doublet $|\pm 2\rangle$ of six magnetically nonequivalent Fe^{2+} centers. The zero field splitting between the quasi-doublet levels $\Delta = 30.9$ GHz, the value of the g -factor $g_z = 2.125$ and the deviations of the principal magnetic z -axes from the crystallographic c -axis of these centers $\beta = 70^\circ$ are determined.

Acknowledgements The authors are grateful to V.D. Scherbakov for supplying us with the sample of natural amethyst and to V.A. Shustov for the X-ray diffraction study of the sample. The measurements were carried out at equipment of Distributed Spectral-Analytical Center of Shared Facilities for Study of Structure, Composition and Properties of Substances and Materials of FRC Kazan Scientific Center of RAS. The work was performed with the financial support from the government assignment for FRC Kazan Scientific Center of RAS.

Author Contributions V.F. Tarasov—wrote drafts of the manuscript. R.B. Zaripov—EPR measurements. All authors reviewed and edited the manuscript.

Funding The work was performed with the financial support from the government assignment for FRC Kazan Scientific Center of RAS. ID 122011800133–2.

Availability of Data and Materials Not applicable.

Declarations

Conflict of Interests The authors declare that they have no known competing financial interests or personal relationships that could have appeared to influence the work reported in this paper.

Ethical Approval Not applicable.

References

1. T.I. Barry, P. McNamara, W. Moore, *J. Chem. Phys.* **42**, 2599 (1965)
2. G. Lehmann, W.J. Moore, *J. Chem. Phys.* **44**, 1741 (1966)
3. R.T. Cox, *J. Phys. C Solid State Phys.* **10**, 4631 (1977)
4. G. Lehmann, H.U. Bambauer, *Angew. Chem. Int. Edit.* **12**, 283 (1973)
5. G. Lehmann, *Am. Miner.* **60**, 335 (1975)
6. C.T. Dotto, S. Isotani, *Radiat. Eff. Defects Solids* **117**, 355 (2006). <https://doi.org/10.1080/10420159108220755>
7. A.J. Cohen, F. Hassan, *Am. Miner.* **59**, 719 (1974)
8. A.J. Cohen, *Am. Miner.* **60**, 338 (1975)
9. G. Cressey, C.M.B. Henderson, G. van der Laan, *Phys. Chem. Miner.* **20**, 111 (1993)
10. P.F. Schofield, C.M.B. Henderson, G. Cressey, G. van der Laan, *J. Synchrotron Rad.* **2**, 93 (1995)
11. S.K. Dedushenko, I.B. Makhnina, A.A. Mar'in, V.A. Mukhanov, Y.D. Perfiliev, *Hyperfine Interact.* **156**, 417 (2004)
12. M. Czajka, M. Kądziołka-Gaweł, A. Konefał, R. Sitko, E. Teper, Z. Mazurak, M. Sachanbinrsk, *Phys. Chem. Miner.* **44**, 365 (2017). <https://doi.org/10.1007/s002R69-016-0864-z>
13. R.T. Cox, *J. Phys. C Solid State Phys.* **9**, 3355 (1976)

14. V.F. Tarasov, R.B. Zaripov, V.D. Scherbakov, *Appl. Magn. Reson.* **54**, 679 (2023). <https://doi.org/10.1007/s00723-023-01545-8>
15. V.F. Tarasov, G.S. Shakurov, *Appl. Magn. Reson.* **2**, 571 (1991)
16. J.A. Weil, *Appl. Mag. Reson.* **6**, 1 (1994)
17. J.S. Griffith, *Phys. Rev.* **132**, 316 (1963)

Publisher's Note Springer Nature remains neutral with regard to jurisdictional claims in published maps and institutional affiliations.

Springer Nature or its licensor (e.g. a society or other partner) holds exclusive rights to this article under a publishing agreement with the author(s) or other rightsholder(s); author self-archiving of the accepted manuscript version of this article is solely governed by the terms of such publishing agreement and applicable law.